Characterising Dependency in Computer Networks using Spectral Coherence

Alex J. Gibberd*, Jordan Noble, Edward A.K. Cohen*

November 28, 2017

Abstract

The transmission or reception of packets passing between computers can be represented in terms of time-stamped events and the resulting activity understood in terms of point-processes. Interestingly, in the disparate domain of neuroscience, models for describing dependent point-processes are well developed. In particular, spectral methods which decompose second-order dependency across different frequencies allow for a rich characterisation of point-processes. In this paper, we investigate using the spectral coherence statistic to characterise computer network activity, and determine if, and how, device messaging may be dependent. We demonstrate on real data, that for many devices there appears to be very little dependency between device messaging channels. However, when significant coherence is detected it appears highly structured, a result which suggests coherence may prove useful for discriminating between types of activity at the network level.

1 Introduction

Understanding how devices on computer networks communicate is a challenging task. While it is possible to gather vast quantities of data from such networks, for instance via packet monitoring, it is difficult to store, let alone process. As a result, protocols such as NetFlow which sample and summarise packet level data are now very popular [1]. Even still, regular monitoring protocols can produce hundreds of gigabytes of summary statistics on a network per day which need to be converted into actionable insights for network administrators.

Network defenders should be at a theoretical advantage over attackers, in that they can attempt to model and understand the day-to-day activity of their network. From such models they can then define what anomalous, and/or malicious events may look like. Additionally, in order to enhance detection performance, one may desire to use prior knowledge of what benign network activity should look like in order to define anomalies. For example, and relevant to the

*Funded by EPSRC grant EP/P011535/1

approach developed here, one may expect that communication between pairs of devices are not correlated such that their activity should be broadly independent when monitored at a network level. However, if traffic is dependent across pairs then this may indicate potentially malicious behaviour such as lateral movement or tunnelling [2].

There are a great variety of measures and methods that can be used to analyse dependency between streams, for instance through measures such as covariance [3], correlation [2], partial correlation [4], or higher-order measures such as cross-cumulants [5]. A traditional approach to network traffic modelling is to assume it is generated according to a Poisson point process [1, 6]. While such models may be generalised to a multivariate setting [7], they do not allow for us to encode auto-correlation structure within a point-process. As a result, we may be able to describe processes which are dependent on each other across data-streams, but they do not allow for dependency within a data-stream itself. When considering computer network traffic, it is not hard to imagine that events from a device will be somehow dependent on previous events from that same device. Spectral approaches, based on either Fourier [8] or time-scale wavelet analysis [9, 10] of processes provide a valuable tool in this situation as they allow for both a rich description of auto-correlation and cross-channel dependency [11].

In this paper, we propose to utilise a measure known as spectral coherence [12] to characterise dependency between network communication channels. We are not aware of any previous application of such a measure to network traffic analysis, although the method has received great attention in neuroscience for modelling neuron dependency [13].

2 Dataset and Preprocessing

Consider network connected devices A, B, C and their associated users, for example, these may be personal computers, DNS servers, authentication servers, or even printers. Typically, we would expect these devices to go about their work as fairly independent actors, i.e. they may browse websites, download material etc., but not in any particularly coordinated manner. Device communication is typically performed through packet transmission. However, given network monitoring limitations, the events that we analyse need not necessarily be packets themselves. More likely, they are aggregates or summaries of communication, for example NetFlow sessions.

In our case, we analyse a subset of NetFlow session data from the Los Alamos National Laboratory (LANL) multi-source cyber-security events data [14, 15]. More specifically, we create a subset of events (NetFlow session start times) relating to the top $N_{\text{triple}} = 500$ busiest edge-pairs in the network over a single day's (Thursday) worth of data. We assess dependency in a pair-wise manner such that data-streams correspond to directed edge-communication between devices $A \to B$ and $B \to C$ for $i = 1, \ldots, N_{\text{triple}}$ device triples $(A, B, C)_i$. For each triple, the activity for each edge corresponds to the same time frame. The protocol monitored is the same for all edge pairs. To avoid confusion, we exclude all flows from the triple (C, B, A) when the triple (A, B, C) is included. One should note that our selection criteria for data-set construction does not explicitly specify devices which have a particular function on the network. However, if we look at the graph of communication edges in Figure 1 it appears that many of our triples have repetitive edges, there are only 95 unique devices in our data-set and 96 unique edges. Looking at the topology of the network it appears that most of the devices are communicating through the device C5721, while we do not have labelled data relating to the function of devices, it would appear that this node acts as some form of server.

We note that in our recordings it is possible to observe two events which have the same start time. This means that the events cannot reasonably be treated as being observed in continuous time, and indeed the timestamps provided with our data are only accurate to the second. As such, the raw events are aggregated into bins of width $\Delta = 1$s. The binned bivariate process will be denoted $\{\boldsymbol{X}[k] = [X_{AB}[k], X_{BC}[k]]^T; k \in \mathbb{Z}\}$, for which we observe a portion $\boldsymbol{X}[1], \boldsymbol{X}[2], ..., \boldsymbol{X}[K]$. As a pre-processing step, we subtract the empirical mean of the data-streams, relabeling $\boldsymbol{X}[k] := \boldsymbol{X}[k] - \bar{\boldsymbol{X}}$ so that they can be well approximated as zero-mean processes.

3 Spectral Coherence as a Measure of Association

In this section, we will define the spectral coherence as a property relating to the cross-spectrum of a bivariate process. The discussion here will be developed based on the understanding that we are with observations relating to a discrete-time process. However, it is also possible to perform such analysis at the individual event level, for examples, see the work of [11, 13, 16].

To simplify the notation, let us use $X_1[k] \equiv X_{AB}[k]$ and $X_2[k] \equiv X_{BC}[k]$. Furthermore, we will assume that $\{X_1[k], X_2[k]\}$ represent a jointly second-order stationary process, i.e. the covariance $\Sigma_{ij}[\tau] \equiv \mathrm{Cov}(X_i[k+\tau], X_j[k])$ only depends on τ for $i, j = 1, 2$. Provided $\sum_\tau |\Sigma_{ij}[\tau]| < \infty$, then for all frequencies $|\omega| \leq \pi/\Delta$, the function $S_{ij}(\omega) = \Delta \sum_{\tau=-\infty}^{\infty} \Sigma_{ij}[\tau] e^{-i\omega\tau\Delta}$, $i, j = 1, 2$, is termed the spectum of $\{X_i[k]\}$ when $i = j$, and the *cross-spectrum* between $\{X_1[k]\}$ and $\{X_2[k]\}$ when $i \neq j$. These spectra can be conveniently represented with the spectral matrix $\boldsymbol{S}(\omega) = (S_{ij}(\omega))$. The argument we present in this paper, is that the cross-spectrum provides a rich framework within which we may characterise computer network messaging processes. In particular, since we are interested in dependency between data-streams, we will concern ourselves with the squared coherencey, or ordinary coherence, defined as the real-valued quantity

$$R(\omega) = \frac{|S_{12}(\omega)|^2}{S_{11}(\omega) S_{12}(\omega)} \ . \tag{1}$$

The coherence provides a useful statistic for assessing dependency between point-processes; not only does it permit a decomposition over frequencies al-

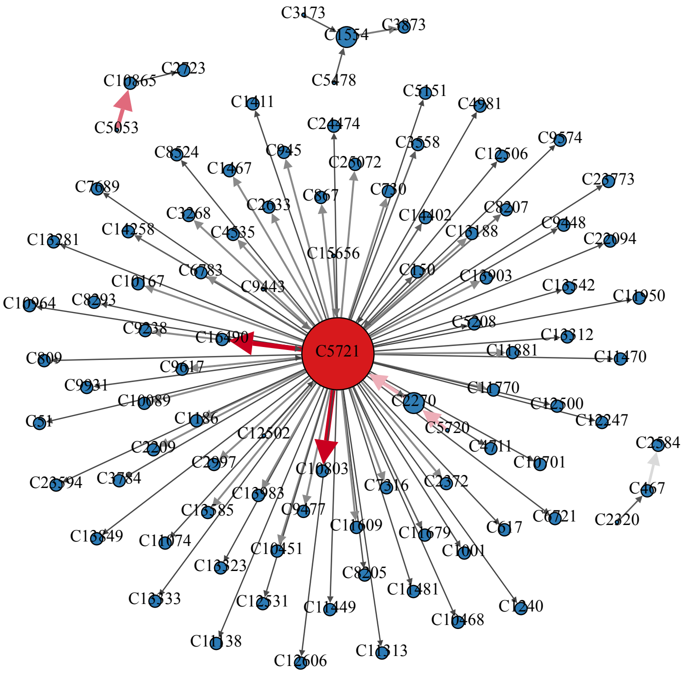

N_{triple}	500	Average length T	17.2 (hours)
Number of nodes	95	Average rate λ_{AB}	0.101 (1/s)
Unique edges	96	Average rate λ_{BC}	0.032 (1/s)

Figure 1: Graph of messaging channels under analysis. Size of text and node are respectively proportional to the out-going and in-going degree. The weight of the edges (and colour) is proportional to the rate measured on that edge.

lowing one to highlight periodicities associated with dependence, but is also invariant to scaling of the marginal auto-covariance as the measure is normalised by the on-diagonal spectra.

3.1 Estimating the Spectra of Point-Processes

Since the true values of the spectra, cross-spectra and coherence are unknown to us, we are required to estimate them from data. The approach that we utilise here is based on the work of Thomson [17]. Specifically, we will construct our estimators from the *tapered discrete-time Fourier transform (tDFT)* defined as

$$\hat{F}_{j;l}(\omega) \equiv \Delta^{1/2} \sum_{k=1}^{K} h_l[k] X_j[k] e^{-i\omega k \Delta} \quad j = 1, 2, \tag{2}$$

for frequencies $-\pi/\Delta < \omega < \pi/\Delta$ where $\{h_l[k]; k = 1, ..., N\}$ for $l = 1, \ldots, L$ are a set of taper sequences. The tapers in the above construction are important, in that they enable us to selectively transform data-points prior to taking the Fourier transform.

If we temporarily assume that $h_l[k] = 1$ for all l, k, then taking the conjugate outer-product leads to the periodogram $\hat{I}_{ij;l}(\omega) \equiv \hat{F}_{i;l}(\omega)\hat{F}^*_{j;l}(\omega)$. Unfortunately, while the periodogram is an asymptotically unbiased estimator of the spectrum $E[\hat{I}_{ij;l}(\omega)] \to S_{ij}(\omega)$ as $T \to \infty$, it is not consistent, in that $\mathrm{Var}[\hat{I}_{ij;l}(\omega)] \not\to 0$. Principally, this is due to us attempting to estimate the spectra at an infinite number of frequencies $\omega \in \mathbb{R}$ with only a finite portion of data [16, 13].

There are several approaches which can be used to sculpt asymptotically consistent estimators of the spectra [18, 17, 19]. A general strategy [19], is to adapt the direct spectral estimate (where $h_l[k] = 1$) such that the tapers take different shapes, for example they may be supported in disjoint regions [8], or constitute a set of overlapping windows [18]. From the Fourier transform of the tapered data, we may then construct vectors $\hat{\boldsymbol{F}}_l(\omega) = [\hat{F}_{1;l}, \hat{F}_{2;l}]^T$ and compute what is known as a *multi-taper spectral estimator* by averaging:

$$\hat{\boldsymbol{S}}(\omega) = \frac{1}{L}\sum_{l=1}^{L} \hat{\boldsymbol{F}}_l(\omega)\hat{\boldsymbol{F}}_l^H(\omega) \quad i, j = 1, 2,$$

where ^{H} denotes the complex conjugate transpose. From the multi-taper spectral estimate we may then obtain an estimate for the coherence $\hat{R}_{12}(\omega)$ via (1) replacing the true spectra $S_{11}(\omega)$, $S_{22}(\omega)$ and $S_{12}(\omega)$ with the estimates $\hat{S}_{11}(\omega)$, $\hat{S}_{22}(\omega)$ and $\hat{S}_{12}(\omega)$, respectively.

3.2 Taper Specification

If we consider choosing orthogonal taper sequences whereby $\sum_k h_l[k]h_{l'}[k] = 0$ for $l \neq l'$ then the resultant Fourier transforms will be asymptotically independent [8]. Averaging over these independent sequences can then reduce the variation in the estimate, the reduction will be related to the number of tapers we average over. It has been demonstrated, c.f. [8], that in the case of asymptotically orthogonal tapers, the sampling distribution of the spectral matrix $\hat{\boldsymbol{S}}(\omega) = (\hat{S}_{ij}(\omega))$ is given by a 2D complex Wishart distribution $\hat{\boldsymbol{S}}(\omega) \sim W_2^C(L, \boldsymbol{S}(\omega))$ with L degrees of freedom and scale matrix $\boldsymbol{S}(\omega)$.

In our application, we utilise a form of taper first demonstrated for spectral estimation by Thomson [17]. Often referred to as the Slepian tapers, these sequences have the beneficial properties that they are mutually orthogonal while maximising energy concentration in a small frequency interval $[-\omega_W, \omega_W]$. If two frequencies are separated by more than this bandwidth, then the bias due to tapering is in some sense minimised. However, as the number of tapers L increases, the width of the side-lobe associated with the Fourier transform of $h_L[k]$ necessarily increases. As such, there is a classic bias-variance trade-off, increasing L reduces the variance, but increases bias. The appropriate number

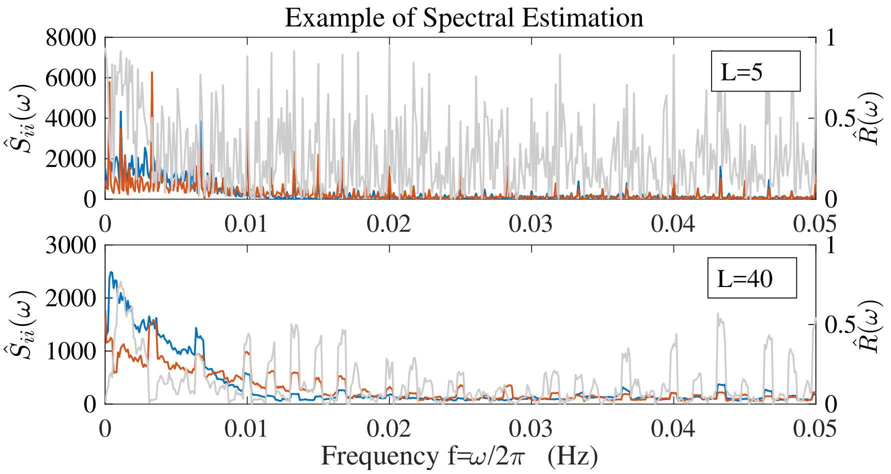

Figure 2: Example of estimates for the spectral density. Top: estimation with $L = 5$ tapers. Bottom: estimation with $L = 40$ tapers. The red and blue lines respectively illustrate the on-diagonal spectral density $\hat{S}_{AB,AB}(\omega)$ and $\hat{S}_{BC,BC}(\omega)$. The grey line indicates the resultant coherence $\hat{R}(\omega)$.

of tapers to use is highly dependent on application and something we will shortly revisit in the context of the network traffic dataset.

4 Dependency in Network Traffic

Applying coherence estimation to edge pairs results in a set of estimates $\{\hat{R}^{(n)}(\omega_1, \ldots, \omega_{N_f})\}$ for $n = 1, \ldots, N_{\text{triple}}$. As may be expected there is significant variation of the spectra across the set of edge-pairs. In this analysis, we consider fixing the window of frequencies such that $\omega_q = 2\pi f_{\max}(q/N_f)$ for $q = 1, \ldots, N_f = 500$ and $f_{\max} = 0.05Hz$. As the length of the edge-pair recordings differ, one may desire to increase L as a function of length T. Potentially, this would lead to increased confidence in our spectral estimate as the Wishart degrees of freedom are increased. However, such an adaptive tapering scheme where L depends on T creates challenges when comparing across coherence estimates as it may be hard to disentangle differences due to the tapering treatment from underlying differences in the process spectra. As such, in these experiments we decide to fix the number of tapers at a moderate level $L = 40$ for all edge-pairs. The difference between tapering with $L = 5$ and $L = 40$ is demonstrated in Figure 2. Note, that while the cross-spectra for different edge-pairs may be of a different scale, the coherence (plotted in grey) provides an intuitive measure on $[0, 1]$ allowing comparison across many data-stream pairs. As an aside, the individual spectra appear non-Poisson, exhibiting shapes that are characteristic of self-exciting behaviour [20].

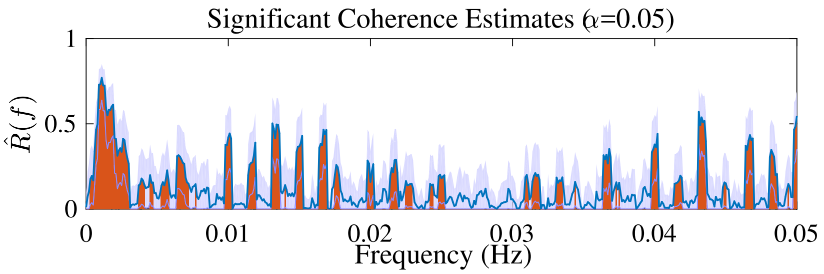

Figure 3: The coherence as plotted in the bottom of Fig. 2 with two-sided 95% confidence intervals. Frequencies where the confidence interval excludes zero are highlighted in red.

Acknowledging that there will be some error in our spectral estimates, it is desirable to assign some measure of confidence to estimates. A useful corollary of the Wishart asymptotic result for multi-taper estimates is that the coherence is distributed (asymptotically) according to the Goodman distribution [12, 21]. Based on this distribution, there are a variety of tests that one may perform to assess the *significance* of a coherence estimate. For example, one may test the null hypothesis that states $R(\omega_q) = 0$ for each frequency ω_q, $q = 1, \ldots, N_f$. Rather than test explicitly against a null of zero coherence, in this work we construct two sided confidence intervals in a similar manner to Wang et al. [22]. Examples of such intervals for $\alpha = 0.05$ are reported in Fig. 3. Alongside these intervals denoted $[\hat{a}_{\alpha/2}, \hat{a}_{1-\alpha/2}]$, we declare that the coherence at a frequency is significant if the interval excludes zero. For this particular triple, we note what appears to be significant coherent beaconing across the devices at multiples of approx. 0.0017Hz (a periodicity of 10 minutes).

To assess variation in coherence estimates across the $N_{\text{triple}} = 500$ edge-pairs under study we attempt to cluster the resultant coherence estimates. Prior to performing clustering, we threshold coherence estimates according to the confidence intervals such that $\hat{R}^*(\omega_q) = 0$ if $0 \in [\hat{a}_{\alpha/2}, \hat{a}_{1-\alpha/2}]$ and $\hat{R}^*(\omega_q) = \hat{R}(\omega_q)$ otherwise. The resultant coherence estimates are then modelled as a *Gaussian mixture model (GMM)*, such that $[\hat{R}^*(\omega_1), \ldots, \hat{R}^*(\omega_{N_f})] \sim \text{GMM}(\{\boldsymbol{\mu}_c, \boldsymbol{\Sigma}_c\}_{c=1}^{C})$ where $\boldsymbol{\mu}_c \in \mathbb{R}^{N_f}$ represent cluster means and $\boldsymbol{\Sigma}_c$ the cluster covariances.

While the Gaussian assumption of the above model contrasts with the Goodman asymptotic distribution for the coherence, the approximation may still hold relevance. For instance, Enochson and Goodman [23] demonstrated that a Gaussian approximation may be effective when calculating confidence intervals. In this example we use the MATLAB implementation of the expectation-maximisation with covariance regularisation set at $\lambda = 0.001$. Due to the many local-minima that may be obtained when fitting a GMM, we perform one thousand replications with random initialisation and report the clustering with the largest likelihood. Figure 4 presents the resulting mean profiles of $C = 4$ clusters alongside the standard-deviation obtained from the estimated covariance

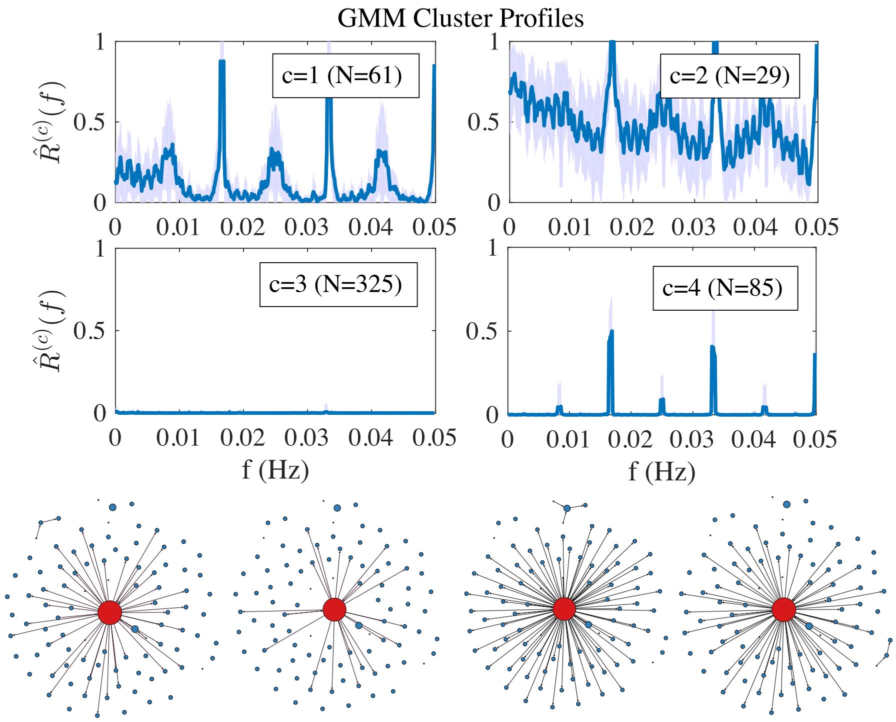

Figure 4: GMM clustering of the significance thresholded coherence estimates with $C = 4$. Shaded regions indicate points within one standard-deviation from the cluster mean. Bottom: graph of edges relating to each cluster $c = 1, 2, 3, 4$ from left to right.

matrices.

5 Discussion

The clustering results are insightful in that the emergence of clusters $c = 3, 4$ partially confirm our initial hypothesis that many device pairs exhibit little dependency. Out of the initial 500 edge-pairs 90 are placed into clusters with non-negliable coherence, for reference, the example demonstrated in Fig. 2 is placed into cluster $c = 1$. These active coherent clusters exhibit pronounced structure across multiple frequencies, once again providing evidence that modelling auto-covariance within network traffic is important. Of some note, is the clear peak at $f = 0.018Hz$ corresponding to periodicity of around 57s . Without a more intimate knowledge of device functionality on the network we can only hypothesise the cause of such a feature, but it is possible this is due to beaconing activities. Interestingly, Heard et al. [24] demonstrate strong periodicity at this same frequency for devices connecting with dropbox.com. While most beaconing activities are benign, scanning techniques used by intruders may also create similar strongly periodic activity and it is thus of interest to administrators to detect such patterns.

As a direction for future work, it is possible the methods developed here to detect association between event driven data-streams in a defensive context, may also be used as a form of correlation attack, for example to break anonymisation protocols when traffic is transmitted via mixing devices [6]. It may also be of interest to relax the stationarity assumptions of this work, for instance within a wavelet framework. Indeed an algorithm that could derive the coherence in a streaming manner would be an important step towards building a practical anomaly detector.

References

[1] N. Duffield, "Sampling for Passive Internet Measurement: A Review," *Statistical Science*, vol. 19, no. 3, pp. 472–498, 2004.

[2] J. Neil, C. Hash, A. Brugh, M. Fisk, and C. C. B. Storlie, "Scan Statistics for the Online Detection of Locally Anomalous Subgraphs," *Technometrics*, vol. 55, no. 4, pp. 403–414, 2013.

[3] S. Jin, D. S. Yeung, and X. Wang, "Network intrusion detection in covariance feature space," *Pattern Recognition*, vol. 40, no. 8, pp. 2185–2197, 2007.

[4] A. Gibberd, M. Evangelou, and J. D. Nelson, "The Time-Varying Dependency Patterns of NetFlow Statistics," in *IEEE International Conference on Data Mining Workshops, ICDMW*, pp. 288–294, 2017.

[5] D. Brillinger, "Moments, Cumulants, and Some Applications to Stationary Random Processes," tech. rep., University College Berkley, 1993.

[6] S. J. Murdoch and P. Zieliński, "Sampled Traffic Analysis by Internet-Exchange-Level Adversaries," *Privacy Enhancing Technologies*, pp. 167 – 183, 2007.

[7] N. Baurele and R. Grubel, "Multivariate Counting Processes: Copulas and Beyond," *Astin Bulletin*, vol. 35, no. 2, pp. 379–408, 2005.

[8] D. R. Brillinger, *Time Series: Data Analysis and Theory.* Philadelphia: SIAM, 1981.

[9] R. H. Riedi, M. S. Crouse, V. J. Ribeiro, and R. G. Baraniuk, "A multifractal wavelet model with application to network traffic," *IEEE Transactions on Information Theory*, vol. 45, no. 3, pp. 992–1018, 1999.

[10] A. Scherrer and N. Larrieu, "Non-gaussian and long memory statistical characterizations for internet traffic with anomalies," *Dependable and . . .* , vol. 4, no. 1, pp. 56–70, 2007.

[11] E. A. K. Cohen, "Multi-wavelet coherence for point processes on the real line," *ICASSP, IEEE International Conference on Acoustics, Speech and Signal Processing - Proceedings*, no. 2, pp. 2649–2653, 2014.

[12] G. Carter, "Coherence and time delay estimation," *Proceedings of the IEEE*, vol. 75, no. 2, pp. 236–255, 1987.

[13] M. R. Jarvis and P. Mitra, "Sampling Properties of the Spectrum and Coherency of Sequences of Action Potentials," *Neural Computation*, vol. 749, pp. 717–749, 2001.

[14] A. D. Kent, "Comprehensive, Multi-Source Cyber-Security Events." Los Alamos National Laboratory, 2015.

[15] A. D. Kent, "Cybersecurity Data Sources for Dynamic Network Research," in *Dynamic Networks in Cybersecurity*, Imperial College Press, June 2015.

[16] D. R. Brillinger, "The spectral analysis of stationary interval functions," *Proceedings of the Sixth Berkeley Symposium on Mathematical Statistics and Probability, Volume 1: Theory of Statistics*, pp. 483–513, 1972.

[17] D. J. Thomson, "Spectrum Estimation and Harmonic Analysis," *Proceedings of the IEEE*, vol. 70, no. 9, 1982.

[18] A. Nuttall and G. Carter, "Spectral estimation using combined time and lag weighting," *Proceedings of the IEEE*, vol. 70, no. 9, pp. 1115–1125, 1982.

[19] A. T. Walden, "A unified view of multitaper multivariate spectral estimation," *Biometrika*, vol. 87, no. 4, pp. 767–788, 2000.

[20] A. G. Hawkes, "Spectra of Some Self-Exciting and Mutually Exciting Point Processes," *Biometrika*, vol. 58, no. 1, pp. 83–90, 1971.

[21] N. R. Goodman, "Statistical Analysis Based on a Certain Multivariate Complex Gaussian Distribution (An Introduction)," *The Annals of Mathematical Statistics*, vol. 34, no. 1, pp. 152–177, 1963.

[22] S. Wang and M. Tang, "Exact confidence interval for magnitude-squared coherence estimates," *Signal Processing Letters, IEEE*, vol. 11, no. 3, p. 326, 2004.

[23] L. Enochson and N. Goodman, "Gaussian approximations to the distribution of sample coherence," *Technical Report*, no. June, 1965.

[24] N. Heard, P. Rubin-Delanchy, and D. J. Lawson, "Filtering automated polling traffic in computer network flow data," *Proceedings - 2014 IEEE Joint Intelligence and Security Informatics Conference, JISIC 2014*, pp. 268–271, 2014.